

# Four-point probe resistivity noise measurements of GaSb layers

L. CIURA<sup>1\*</sup>, A. KOLEK<sup>1</sup>, D. SMOCZYŃSKI<sup>2</sup>, and A. JASIK<sup>2</sup>

<sup>1</sup>Department of Electronics Fundamentals, Rzeszow University of Technology, W. Pola 2, 35-959 Rzeszow, Poland

<sup>2</sup>The Łukasiewicz Research Network – Institute of Electron Technology, Al. Lotników 32/46, 02-668 Warsaw, Poland

**Abstract.** This paper concerns measurements and calculations of low frequency noise for semiconductor layers with four-probe electrodes. The measurements setup for the voltage noise cross-correlation method is described. The gain calculations for local resistance noise are performed to evaluate the contribution to total noise from different areas of the layer. It was shown, through numerical calculations and noise measurements, that in four-point probe specimens, with separated current and voltage terminals, the non-resistance noise of the contact and the resistance noise of the layer can be identified. The four-point probe method is used to find the low frequency resistance noise of the GaSb layer with a different doping type. For n-type and p-type GaSb layers with low carrier concentrations, the measured noise is dominated by the non-resistance noise contributions from contacts. Low frequency resistance noise was identified in high-doped GaSb layers (both types). At room temperature, such resistance noise in an n-type GaSb layer is significantly larger than for p-type GaSb with comparable doping concentration.

**Key words:** low frequency noise, GaSb noise, noise measurements, resistance noise calculations.

## 1. Introduction

The semiconductor layers, which are commonly electrically characterized by manifesting resistance, can also be characterized by the resistance low frequency noise. It is a nontrivial electrical property, which includes both  $1/f$  and generation-recombination (g-r) noise types. From low frequency noise, additional knowledge about properties of a semiconductor layer can be gained, i.e. the connection of the  $1/f$  or g-r noise with defects in a material is well known [1, 2].

Noise characterization of the semiconductor layer requires sensitive measurement techniques. Such layers have distinctly smaller low frequency noise than a device with a depletion region [3]. Using such sensitive methods does not guarantee characterization of the semiconductor layer itself, due to the influence of the contact, i.e. metal/semiconductor interface noise. These undesired excess contributions should be removed, or at least identified when low frequency noise properties of a semiconductor material need to be characterized. The contact-related low frequency noise can be evaluated with the four-point probe noise measurements method. The method can be applied to the same samples used in Hall effect measurements, so there is no need to prepare special samples/devices for noise experiments.

This paper focuses on the identification of layer- and contact-related low frequency noise by means of the four-point probe method. Such identification requires measurements supported by numerical calculations for result interpretation. The gallium antimonide (GaSb) layers were chosen for the

four-probe method illustration. Gallium antimonide is one of the key materials for infrared technology. It is lattice-matched to many compounds of the III–V group as well as to superlattices, which cover a wide spectral range of infrared radiation. Therefore GaSb can be used as a substrate [4] or as a component [5, 6] for the fabrication of high-quality infrared detectors. The GaSb material research covering physics and technology has been reviewed by Dutta et al. [7]. However, the low frequency noise properties of GaSb have not been investigated so far.

## 2. Experiment

The GaSb layers used in this study were deposited on a semi-insulating GaAs substrate using the interfacial misfit array growth method. Thickness of the GaSb layers was in the range of 1–1.3  $\mu\text{m}$ . The samples were p-doped with beryllium or n-doped with tellurium. Three p-doped and two n-doped samples with different measured carrier concentrations were analyzed. In p-type specimens, the carrier concentrations were:  $1 \times 10^{17} \text{ cm}^{-3}$ ,  $7 \times 10^{17} \text{ cm}^{-3}$  and  $5 \times 10^{18} \text{ cm}^{-3}$ , and in n-type specimens they stood at  $2 \times 10^{16} \text{ cm}^{-3}$  and  $7 \times 10^{17} \text{ cm}^{-3}$ . The squared samples (5 mm  $\times$  5 mm) were manufactured originally for Hall effect measurements. The four indium-based contacts ( $\text{In}_{95\%}\text{Zn}_{5\%}$ ) are located near the sample corners.

The low frequency noise properties of GaSb layers can be determined from voltage or current noise measurements. However, for low resistive layers, measurements of voltage noise instead of current noise are preferred. The influence of the equivalent input current noise of the voltage amplifier is negligible for the low resistive device under test (DUT). Additionally, the uncorrelated equivalent input voltage noise of the amplifier can be effectively reduced by cross-spectral density

\*e-mail: lciura@prz.edu.pl

Manuscript submitted 2019-07-08, revised 2019-09-13, initially accepted for publication 2019-09-29, published in February 2020

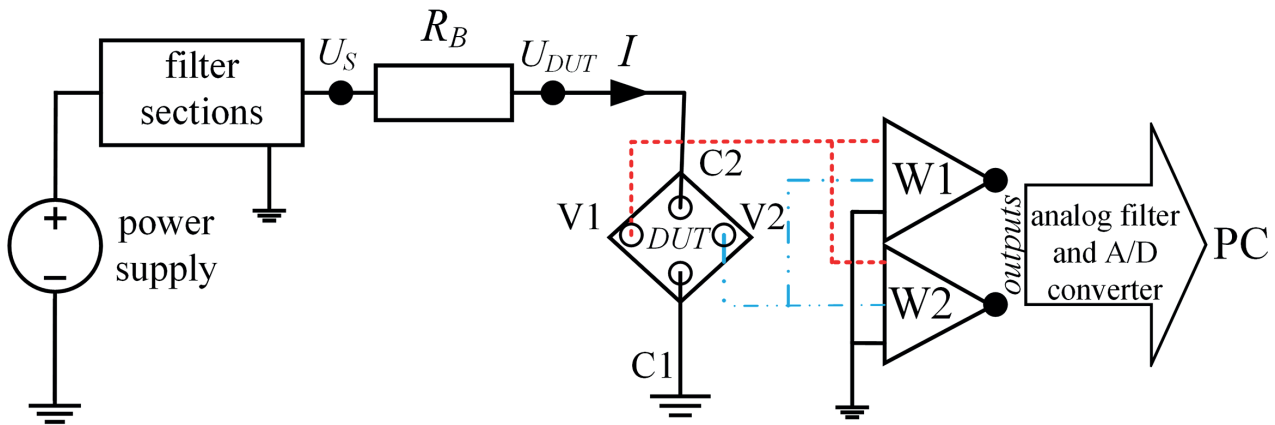


Fig. 1. Voltage noise measurements setup for semiconductor layer with four electrodes

calculation [8]. This method is easier to implement with the voltage rather than current amplifiers.

The voltage low frequency noise is measured in the circuit presented in Fig. 1. The DUT is biased with the current provided by the power supply and by resistance  $R_B$ . The value of  $R_B$  satisfies the condition  $R_B \gg R_{DUT}$ , where  $R_{DUT}$  is DUT resistance.

The bias current is constant,  $I = U_s / (R_B + R_{DUT}) \approx I = U_s / R_B$ , where  $U_s$  is the source voltage measured after filter sections, which are used for reducing power supply noise. The voltage  $U_{DUT}$ , across the DUT, is also measured, so the resistance of the DUT can be found:  $R_{DUT} = U_{DUT} / I$ .

There are several ways (configurations) to provide the bias current and acquire voltage signals from four-electrode DUT. The key difference between configurations is discussed in a further section. In Fig. 1, one of the possibilities is presented. The bias current is provided to one pair of the terminals (C1 and C2), which are called current terminals (CT). The remaining pair (V1 and V2), used as sensors, are referred to as voltage terminals (VT). At the voltage terminals, the differential signal is measured with two differential amplifiers (W1 and W2). For such measurements, general-purpose amplifiers can be used. Amplifier W1 is Signal Recovery 5186 while amplifier W2 is a self-made unit. They feature low noise (equivalent input noise voltage of about  $3\text{nV}/\text{Hz}^{1/2}$  at 1 kHz) and have high input impedance ( $100\text{ M}\Omega$ ) as well as wide bandwidth (up to 1 MHz). The amplified signals go to the antialiasing filter and further to the analog/digital (A/D) converter of the acquisition card connected with the computer. The cross-correlation method [8] is applied to the outputs of amplifiers W1 and W2. Such a method allows reducing the uncorrelated noise contributions, namely the equivalent input voltage noise of the two amplifiers. With this method, a DUT signal level 30 dB lower than the background noise of a single amplifier can be measured within acceptable averaging time [9]. The low frequency noise of DUT is found by subtracting the measured cross-spectral density for the unbiased DUT from measurements for the biased DUT.

Typically measured cross-spectral densities are illustrated in Fig. 2. As can be seen, the low frequency noise observed

includes both the  $1/f$  and generation-recombination (g-r) noise with the Lorentzian cross-spectral density shape.

### 3. Calculations

The already mentioned choice of current/voltage terminals (CT/VT) is very important because the measured resistance noise does not come from the entire semiconductor layer. In each configuration of the terminals, the particular regions of the layer have different contributions to the total observed low frequency

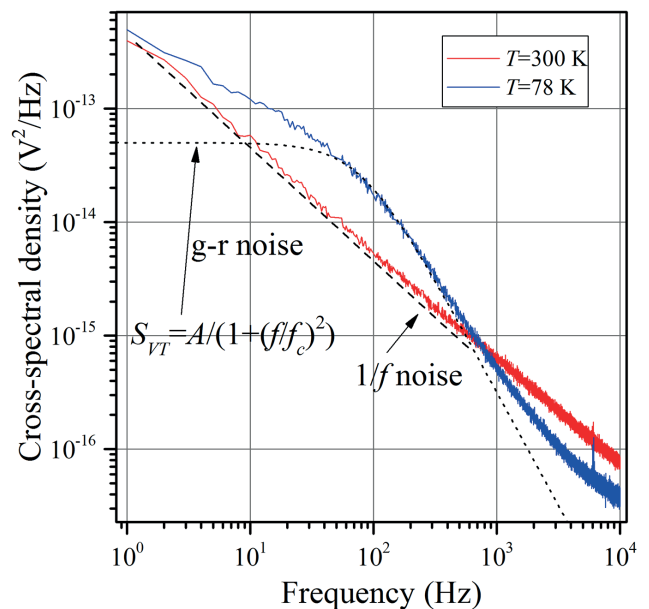


Fig. 2. Measured cross-spectral densities of the voltage noise for the n-type GaSb layer biased with the constant current  $I = 160\ \mu\text{A}$  at two temperatures. Two typical low frequency noise components are indicated:  $1/f$  and Lorentzian shape with corner frequency  $f_c$  and the constant  $A$  related to the g-r noise magnitude

## Four-point probe resistivity noise measurements of GaSb layers

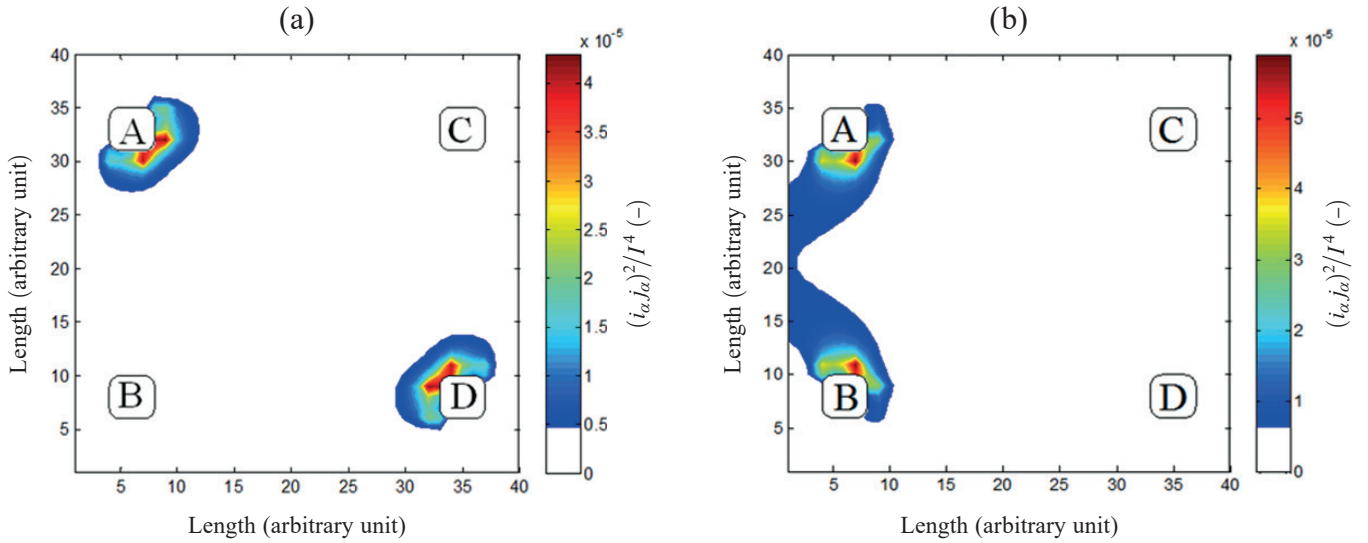


Fig. 3. Calculated gain  $(i_\alpha j_\alpha)^2/I^4$  for the resistance noise when current and voltage terminals are the same. Terminals are AD (Fig. 3a) or AB (Fig. 3b). The white color is assigned for values which satisfy the condition  $(i_\alpha j_\alpha)^2/I^4 < 0.1 \max[(i_\alpha j_\alpha)^2/I^4]$ . The length is in arbitrary units while the gain is dimensionless

noise. Furthermore, the intensity of the total acquired noise also depends on the choice of CT/VT.

The problem of resistance noise measurements with the arbitrarily placed CT and VT on a two/three-dimensional conductor modeled by the resistive network has been solved by Vandamme and Bokhoven [10]. According to their work, the power (or cross) spectral density of voltage fluctuations  $S_{VT}$  measured at VT, when the constant bias current  $I$  is provided for CT, is:

$$S_{VT} = \frac{\sum_{\alpha} (i_{\alpha} j_{\alpha})^2 S_r^{\alpha}}{I^2} \quad (1)$$

where  $i_{\alpha}$  is the local current in  $\alpha$  – branch of the original network, i.e. when current is provided for CT and voltage fluctuations are measured at VT,  $j_{\alpha}$  is the current in the adjoint network, with the roles of CT and VT reversed. Local resistance fluctuations of each branch  $\alpha$  have spectral density  $S_r^{\alpha}$ . Equation (1) is valid only if such fluctuations are spatially uncorrelated (resistance in each branch fluctuates independently). For homogeneous samples, all fluctuations of the resistance in each branch have the same spectral density  $S_r^{\alpha} = S_r$ . In equation (1), the quantity  $S_{VT}$  is proportional to the squared bias current because both branch currents,  $i_{\alpha}$  and  $j_{\alpha}$ , depend on  $I$ . The power/cross spectral density of resistive noise  $S_R$ , defined as:

$$\frac{S_{VT}}{I^2} \equiv S_R = \frac{\sum_{\alpha} (i_{\alpha} j_{\alpha})^2 S_r^{\alpha}}{I^4}, \quad (2)$$

is better for our considerations than  $S_{VT}$  because it includes dimensionless and bias-independent coefficient  $(i_{\alpha} j_{\alpha})^2/I^4$ , which can be interpreted as local gain for the local noise with spectral density  $S_r^{\alpha}$ . The gain determines which area of

the examined layer contributes to the measured cross-spectral density  $S_R$ . The quantity  $S_R$  is not relative but circuit dependent [11] due to dependence on the layer resistance  $R_{DUT}$ . The circuit independent quantity, i.e. the relative noise, requires normalization. This is done in section 4.2 for the sake of comparison of the GaSb low frequency resistance noise.

Gain  $(i_{\alpha} j_{\alpha})^2/I^4$  can be calculated by means of the node voltage method for the geometry and CT/VT configurations of DUT. In the numerical calculations, the DUT is modeled by a two-dimensional homogenous structure (resistive network), which reflects the sample dimensions, contacts' location, and their finite dimensions. The squared contacts are labeled A, B, C and D. In Fig. 3, and Fig. 4, the calculated values of  $(i_{\alpha} j_{\alpha})^2/I^4$  are shown. Bias current  $I$  is taken as unity. In the first case (Fig. 3a), the current is provided to AD terminals, and the noise is measured at the same contacts, so such case can be denoted as  $AD_{CTVT}$ . In this case, the adjoint network is the same as the original one, which means that  $i_{\alpha} = j_{\alpha}$ . The colors in the figures, which represent values, are chosen so that 10% (or lower) of the maximum value was assigned to the white color. This means that the colored area contributes much to the total measured noise. For the  $AD_{CTVT}$  (Fig. 3a) and  $AB_{CTVT}$  (Fig. 3b) configurations, the calculated gain is significantly non-uniform. The highest gain was found for the area near the contacts, which means that the measured low frequency noise is dominated by the contributions from these regions of the layer. For the  $AD_{CTVT}$  (Fig. 3a) configuration, the highest gain is near the corners of the contacts, while for  $AB_{CTVT}$  (Fig. 3b), the highest gain is near the bottom or the top contact's edge. In Fig. 4, the results of the calculations are presented for configurations  $AD_{CT}BC_{VT}$  (Fig. 4a) and  $AB_{CT}CD_{VT}$  (Fig. 4b). If the CT and VT are different terminals, the measured noise is related to the whole layer area, not only to the near-contact region, because the gain is distributed in a more regular manner.

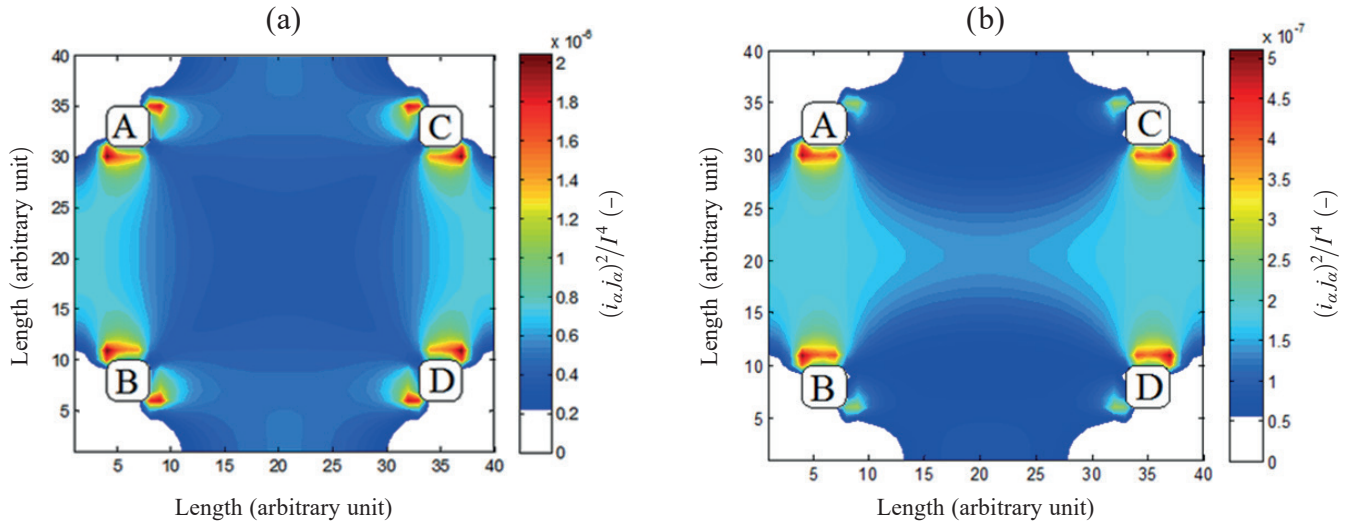


Fig. 4. Calculated gain  $(i_{\alpha} J_{\alpha})^2 / I^4$  for resistance noise. In Fig. 4a, current terminals are AD and voltage terminals are BC. In Fig. 4b current terminals are AB and voltage terminals are CD. The white color is assigned for values which satisfy the condition  $(i_{\alpha} J_{\alpha})^2 / I^4 < 0.1 \max[(i_{\alpha} J_{\alpha})^2 / I^4]$ . The length is in arbitrary units while gain is dimensionless

The configuration with separated CT and VT should be used if resistance fluctuations of the whole layer have to be characterized; however, contributions from the near-contact area remain very prominent. For both configurations, the gain is very small near the sample corners behind the contacts (white color). For the  $AD_{CT}BC_{VT}$  (Fig. 4a) configuration, the highest gain is for the near-contact region but its value is more than one order of magnitude lower than for e.g.  $AD_{CT}VT$ . In the center of the layer, the gain is slightly lower than for the area near the layer edge. For the  $AB_{CT}CD_{VT}$  (Fig. 4b) configuration, the highest gain magnitude is even lower than the highest gain for the previous configuration. The gain has quite uniform distribution in the layer's center.

Configuration  $AD_{CT}BC_{VT}$  (Fig. 4a), with diagonally provided current, seems to be optimum for resistance noise characterization of the layers. The whole sample makes a contribution to the total resistance noise, and the absolute value of  $\sum_{\alpha} (i_{\alpha} J_{\alpha})^2$  is higher than for  $AB_{CT}CD_{VT}$ , which proves very important if the noise of the layer is low.

From Equation (2) and the above calculations (Fig. 3 and 4), one can deduce that changing the role of contacts, e.g. switching configuration  $AD_{CT}BC_{VT}$  to  $BC_{CT}AD_{VT}$ , does not change the calculated value of  $S_R$  if the noise comes from resistance fluctuations of the layer. This is true even when noise sources have no homogeneous distribution in the layer or if several resistance fluctuation mechanisms exist [12]. Deviations from this reciprocity rule indicate some extra non-resistance noise contribution from the contacts, i.e. metal-semiconductor interfaces. The low frequency noise measurements emerge as the sensitive tool for contact evaluation because even for ohmic behavior of the contacts local depletion regions can exist. The depletion regions commonly introduce non-resistance low frequency noise with a high magnitude [3], which immediately breaks the reciprocity rule.

## 4. Results

**4.1. Interpretation.** The calculations in section 3 are useful for the interpretation of experimental results. For cross-spectral density of voltage fluctuations,  $S_{VT}$  was measured for p-doped and n-doped GaSb layers with the setup from Fig. 1 for a number of configurations of CT and VT terminals. The measured cross-spectral densities have the  $1/f$  shape. The magnitude of such noise:  $S_R = S_{VT} / I^2 / f$  at  $f = 1$  Hz versus temperature is shown in Fig. 5 for the n-type layer doped to  $2 \times 10^{16} \text{ cm}^{-3}$  (Fig. 5a) and for the p-type layer doped to  $1 \times 10^{17} \text{ cm}^{-3}$  (Fig. 5b).

For both layers in two-probe configurations (CT is also VT), the measured characteristics  $S_R(1000/T)$  significantly depend on the choice of the contact. As can be seen in Fig. 5, the reciprocity rule is generally not fulfilled in both cases, e.g. noise measured in the  $AD_{CT}BC_{VT}$  configuration is different than in the  $BC_{CT}AD_{VT}$  one. This means that the measured noise for these layers is the non-resistance component, probably introduced by the contacts. The capacitance measurements confirmed that depletion regions exist in the n-doped layer. This was to be expected because making ohmic contact constitutes a challenge for the low n-doped GaSb layer. The layers with higher doping were also evaluated. For the p-type layer doped to  $5 \times 10^{18} \text{ cm}^{-3}$ , no low frequency noise was observed. The results for the n-type layer doped to  $7 \times 10^{17} \text{ cm}^{-3}$  are shown in Fig. 6 for the two-electrode configuration, with curves depending on the choice of the contact. For configuration with separated CT and VT, e.g.  $AD_{CT}BC_{VT}$  and for reciprocal configuration –  $BC_{CT}AD_{VT}$ , the measured noise is the same. The reciprocity rule is obeyed, so the measured noise is indeed the resistance noise of the layer and the contacts do not contribute any non-resistance noise. For configuration  $AB_{CT}CD_{VT}$  the measured value of  $S_R$  is lower. This is expected because for such configuration the value of  $\sum_{\alpha} (i_{\alpha} J_{\alpha})^2$  is lower.

## Four-point probe resistivity noise measurements of GaSb layers

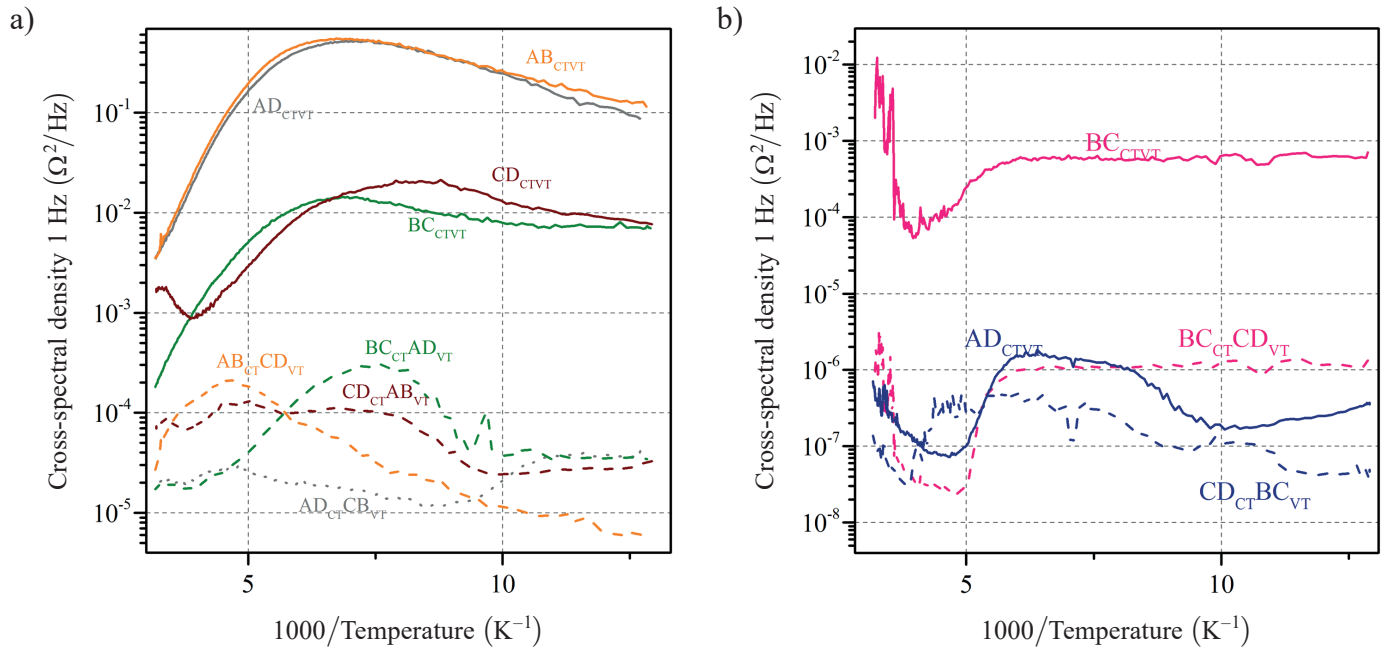


Fig. 5. Cross-spectral density  $S_R = S_{VT}/I^2/f$  at  $f = 1$  Hz versus temperature measured for different configurations of current and voltage terminals for n-GaSb doped to  $2 \times 10^{16} \text{ cm}^{-3}$  (Fig. 5a), and p-GaSb doped to  $1 \times 10^{17} \text{ cm}^{-3}$  (Fig. 5b)

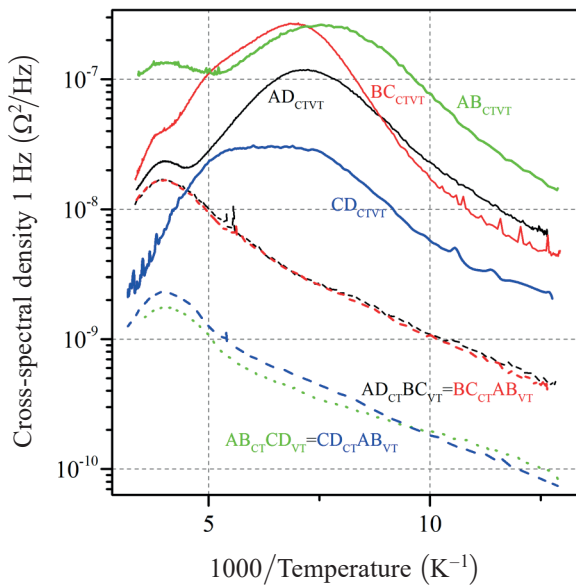


Fig. 6. Cross-spectral density  $S_R = S_{VT}/I^2/f$  at  $f = 1$  Hz versus temperature measured for different configurations of current and voltage terminals for n-type GaSb doped to  $7 \times 10^{17} \text{ cm}^{-3}$

**4.2. Resistance noise of GaSb layers.** The layer-related low frequency resistance noise can be estimated by means of four-point probe measurements with separated current and voltage terminals for specimens which obey the reciprocity rule. Two of such specimens were found: n-type and p-type GaSb layers with approximately the same doping concentration ( $\approx 7 \times 10^{17} \text{ cm}^{-3}$ ). The diagonal configuration ( $AD_{CT}BC_{VT}$ ) of measurements was used to find the quantity of  $S_R$ . Then, the relative low frequency

resistance noise can be found if normalization of  $S_R$  by layer sheet resistance  $R_{sheet}$  (obtained from Hall effect measurements) is performed. The values of  $S_R$  at  $f = 1$  Hz and sheet resistance  $R_{sheet}$  measured at room temperature as well as relative resistance noise,  $L_{lf} \equiv S_R/(R_{sheet})^2$ , are gathered in table I for n-type and p-type GaSb layers. At room temperature, the relative noise of a similarly doped layer is three orders of magnitude higher for n-type than for p-type GaSb. Interestingly, no low frequency noise is observed for the p-type layer doped to  $5 \times 10^{18} \text{ cm}^{-3}$ . This suggests that both the contact and the resistance noise of the layer decrease with increasing doping concentration.

Table 1

Absolute and relative low frequency resistance noise at room temperature for beryllium (p – GaSb) and tellurium (n – GaSb) doped GaSb layers. The doping was roughly the same ( $\approx 7 \times 10^{17} \text{ cm}^{-3}$ )

Layer	Results at room temperature		
	$S_R$ ( $\Omega^2/\text{Hz}$ )	$R_{sheet}$ ( $\Omega/\text{sq}$ )	$L_{lf}$ (1/Hz)
(n – GaSb)	$1.1 \times 10^{-8}$	35	$9 \times 10^{-12}$
(p – GaSb)	$2.3 \times 10^{-10}$	155	$9.7 \times 10^{-15}$

## 5. Conclusions

The four point-probe noise measurements performed with the aid of numerical calculations constitute a valuable technique to study the low frequency resistance noise of any semiconductor layer. With this method, both contact non-resistance noise and layer-related resistance noise can be identified. The contacts can be a source of significant low frequency non-resistance

noise due to the presence of the depletion region. Non-resistance noise violates the reciprocity rule, which is always obeyed for resistance noise. At room temperature, the relative low frequency resistance noise of the GaSb layers with similar doping levels but of different doping types is three orders of magnitude higher for the n-type Te-doped layer than for the p-type Be-doped GaSb layer.

**Acknowledgments.** This work was supported by the National Centre for Research and Development under project No. TECHMATSTRATEG1 /347751/5/NCBR/2017 (TRANSFER).

## REFERENCES

- [1] L.K.J. Vandamme, "Noise as a diagnostic tool for quality and reliability of electronic devices," *IEEE Transactions on Electron Devices* 41(11), 2176–2187, 1994.
- [2] B.K. Jones, "Low-frequency noise spectroscopy," *IEEE Transactions on Electron Devices* 41(11), 2188–2197, 1994.
- [3] T.G.M. Kleinpenning, S.Jarrix, and G. Lecoy, "Generation-recombination noise in submicron semiconductor layers: Influence of the edges," *Journal of Applied Physics* 78(4), 2883–2885, 1995.
- [4] D. Wu, Q. Durlin, A. Dehzangi, Y. Zhang, and M. Razeghi, "High quantum efficiency mid-wavelength infrared type-II InAs/InAs<sub>1-x</sub>Sb<sub>x</sub> superlattice photodiodes grown by metal-organic chemical vapor deposition," *Applied Physics Letters* 114(1), 011104, 2019.
- [5] E. Gomółka, O. Markowska, M. Kopytko, A. Kowalewski, P. Martyniuk, A. Rogalski, J. Rutkowski, M. Motyka, and S. Krishna, "Mid-wave InAs/GaSb superlattice barrier infrared detectors with nBnN and pBnN design," *Bull. Pol. Ac.: Tech.* 66(3), 317–323, 2018.
- [6] Y. Teng, Y. Zhao, Q. Wu, X. Li, X. Hao, M. Xiong, and Y. Huang, "High-Performance Long-Wavelength InAs/GaSb Superlattice Detectors Grown by MOCVD," *IEEE Photonics Technology Letters* 31(2), 185–188, 2019.
- [7] P.S. Dutta, H.L. Bhat, and V. Kumar, "The physics and technology of gallium antimonide: An emerging optoelectronic material," *Journal of Applied Physics* 81(9), 5821–5870, 1997.
- [8] F. Crupi, G. Giusi, C. Ciofi, and C. Pace, "Enhanced Sensitivity Cross-Correlation Method for Voltage Noise Measurements," *IEEE Transactions on Instrumentation and Measurement* 55(4), 1143–1147, 2006.
- [9] C. Ciofi, F. Crupi, and C. Pace, "A new method for high-sensitivity noise measurements," *IEEE Transactions on Instrumentation and Measurement* 51(4), 656–659, 2002.
- [10] L.K.J. Vandamme and W.M.G. van Bokhoven, "Conductance noise investigations with four arbitrarily shaped and placed electrodes," *Applied Physics A* 14(2), 205–215, 1977.
- [11] B. Ayhan, C. Kwan, J. Zhou, L.B. Kish, K.D. Benkstein, P.H. Rogers, and S. Semancik, "Fluctuation enhanced sensing(FES) with a nanostructured, semiconducting metal oxide film for gas detection and classification," *Sensors and Actuators B: Chemical* 188, 651–660, 2013.
- [12] L.K.J. Vandamme and G. Leroy, "Analytical expressions for correction factors for noise measurements with a four-point probe" *Fluctuation and Noise Letters* 6(2), 161–178, 2006.